Developments in High Spatial Resolution Imaging of Faint, Complex Objects at Lowell Observatory

Dr. Gerard van Belle
Lowell Observatory

ABSTRACT

We have been pursuing a comprehensive program of high-resolution imaging at Lowell Observatory, for the purpose of spatially resolved observations of faint objects at scales down to less than 1 milliarcsecond. This activity has had two principal thrusts aimed at improving both spatial resolution and sensitivity of advanced astronomical interferometric imaging techniques. First, we have been building upon our successes with on-sky operations with DSSI (Differential Speckle Survey Instrument) at Lowell's 4.3-meter Lowell Discovery Telescope (LDT), and developing the follow-on QWSSI (Quad-camera Wavefront-sensing Six-Channel Speckle Interferometer). QWSSI simultaneously images in 4 visible and 2 near-infrared narrow bandpasses, while the remaining light feeds a high-sensitivity achromatic wavefront sensor. Second, Lowell has been implementing an upgrade of the Navy Precision Optical Interferometer (NPOI), which is augmenting the telescope array with three AO-assisted 1-meter telescopes. These complementary programs of speckle and long-baseline interferometric observing at LDT and NPOI are intended to work jointly to constrain the low- and high-spatial frequency imaging information of stellar surface structure, stellar multiplicity, and other complex on-sky objects. First light activities associated with these efforts will be presented at AMOS.

1. INTRODUCTION

For an integrated solution to the challenge of imaging high-altitude ($\gtrsim$1,000 miles) satellites, including (but not limited to) geostationary satellites, we are leveraging two major, operational facilities for which Lowell Observatory has privileged access: the observatory's 4.3-m Lowell Discovery Telescope (LDT[1]), and the Navy Precision Optical Interferometer (NPOI). Both of these facilities are operating on-sky *right now* and constitute major infrastructure investments which are being utilized to test and validate many of the techniques necessary for an operational geosat imaging facility. The work at Lowell has been outline in previous AMOS presentations; in [1, 2] we presented the signal-to-noise arguments, and in [3] we discussed the on-sky, *operational* experience of astrophysicists with ground-based facilities in carrying out sub-milliarcsecond angular resolution science.

1.1 Overall System Architecture

The system architecture has the following high-level elements:

1. *Optical interferometry.* Spatial resolution in the sub-arcsecond to single-milliarcsecond regime requires an interferometric telescope array. Observing in the 'optical' – namely, both visible and near-infrared wavelengths – is required to both achieve the spatial resolution, but also to observe the features of interest on geosats.
2. *Reconfigurable array.* Geosats range in spatial scale from 10-200 milliarcseconds (mas), so adjusting the resolving power of the array through reconfiguration is needed. Additionally, a reconfigurable array provides dense access to $\{u,v\}$ data points for image reconstruction.
3. *Baseline bootstrapping.* The desired resolution element size of 10 cm or smaller can be observed with the longest baselines of an interferometric array, but at low signal-to-noise-ratio (SNR); as such, tracking on short baselines with their high SNR is necessary to coherently lock the long baselines.

[1] Formerly known as the Discovery Channel Telescope (DCT).

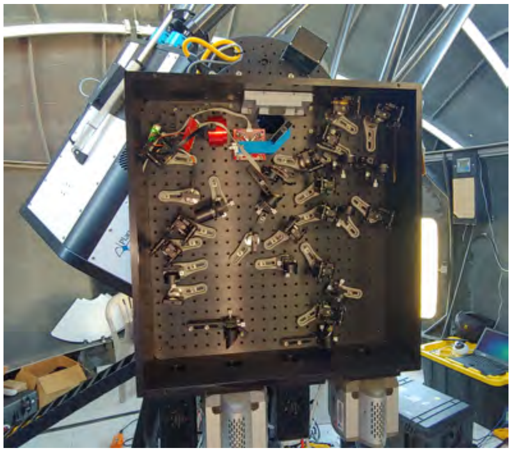

Fig. 1: The QWSSI instrument mounted on NPOI PW1000-1, for first light on Jun 8, 2020 .

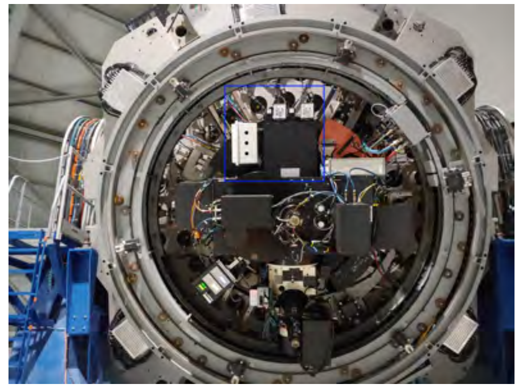

Fig. 2: The QWSSI instrument mounted on the LDT instrument cube (blue box); first light on the 4.3-m was Jul 30, 2020.

4. *Wavelength bootstrapping.* Near-IR fringe tracking (FTK) has two significant (and essential) benefits: first, satellites are brighter in the near-IR than in the visible; second, the lower resolving power of longer wavelength observing means higher SNR for FTK. Both of these benefits increase the ability of an array to be coherently phased on a satellite for integrating ('staring') at visible wavelengths.

5. *Large apertures.* Satellites are faint relative to the current state-of-the-art in optical interferometry; adaptive-optics (AO) corrected apertures of size $\geq$1.0 m are required.

6. *Complementary single-aperture imaging.* Using the technique of speckle imaging, Lowell's 4.3 m LDT effectively can operate as a very-short-baseline optical interferometer and serve to constrain image reconstructions. Of these six elements, items 1-3 and 6 have already advanced to on-sky operations.

The LDT and NPOI facilities has the necessary flexibility for this task of high-altitude satellite imaging, and over the past 24 months, aggressive development has proceeded on all of these fronts. This manuscript documents our progress on all fronts, following an earlier conference proceedings update [4].

2. SINGLE APERTURE SPECKLE DEVELOPMENTS AT LOWELL

2.1 Speckle Imaging at LDT

One of the simplest examples of SSA observing desired for geosats, namely "confirming the successful deployment of solar panels", is already readily obtained from large (> 4 m) single-aperture telescope observations. Using the Differential Speckle Survey Instrument [DSSI, 5], in 2014 we carried out a pilot observational program of geosats and other high-altitude satellites with simultaneous operational wavelengths of 692 nm & 880 nm, resulting in resolving power of 33 mas & 42 mas (see Figure 1 of [1]); this is $\approx$ 7 pixels across large geosats (roughly 6 m resolution at that distance). Although this does not seem like terribly fine resolution, it is indeed sufficient to establish the status of the solar panel deployment on these geosats - not too shabby for an instrument that had a capital investment of $\sim$\$200k for construction from off-the-shelf components. The sensitivity limit for DSSI is $V \approx 15.5$ on the LDT under the best seeing conditions; secondary objects relative to primaries of this brightness can be detected with a brightness difference of $\Delta m = 3.5$ at separations of 200 mas [6], and we have productively utilized DSSI in a variety of science applications [7, 8, 9, 10, 11, 12]. Along with the high resolution imaging, a key observational capability demonstrated in this pilot program was the ability to track highly non-sidereal targets with the LDT at altitudes from 10,000 to 25,000 miles.

Building on our successes with DSSI, we have now developed and deployed the Quad-camera Wavefront-sensing Six-Channel Speckle Interferometer (QWSSI). QWSSI improves upon the DSSI concept in multiple ways.

- Instead of two speckle imaging channels (DSSI operates typically at 692nm and 880nm), QWSSI has four in the visible (577, 658, 808, 880nm), plus two that extend the imaging reach into the near-infrared (1200 and 1500 nm).
- The speckle channels are narrow in bandwidth (20 to 40 nm wide), but unlike DSSI, QWSSI does not discard the out-of-band light but rather carefully manages it for capture by a wavefront sensor. The intent is to implement wavefront-sensor enhanced speckle imaging techniques developed by the Maui group [13, 14] in a civilian setting, enabling and enhancing reconstruction techniques such as Multi-Frame Blind Deconvolution (MFBD) [15].

For engineering tests, we initially deployed QWSSI on the second Nasmyth port of one of our NPOI PW1000 1-m telescopes (Figure 1) in June 2020, followed by first science observing at the LDT (Figure 2) in July 2020. We image the four visible light speckle bandpasses on separate quadrants of an Andor iXon 888 imager, and route the WFS light onto a separate Andor (Figure 7); the two infrared channels are each imaged separately one of two First Light Instruments CRED-2 InGaAs imagers.

3. LONG BASELINE OPTICAL INTERFEROMETRY DEVELOPMENTS AT LOWELL

Current NPOI Status. NPOI is an operational long-baseline optical interferometer, combining up to six beams from independent telescopes. The current small (12 cm) apertures have been used for development of a high-precision astrometric catalog [16], world-first interferometric observations of geosats [17, 18], along with scientific investigations [19, 20, 21, 22, 23, 24, 25, 26, 27, 28, 29, 30]. Recent technical developments include the six-way Visible Imaging System for Interferometric Observations at NPOI (VISION) beam combiner [31, 32], and a updated instrument back end that provides multi-baseline bootstrapping and coherent integration of fringe visibilities [33, 34, 35]. The original detailed instrument paper [36] with a recent update [37] are also available.

In FY17 we began a project to add three 1.0 m telescopes to the NPOI facility. Each of these telescopes is being equipped with adaptive optics, and is relocatable from compact spacings ($\sim$8 m) out to the ends of each vacuum arm for a full 432 m baseline. An InGaAs near-IR fringe tracker will also be installed to stabilize B- and V-band fringes for the existing imagers. The development for these various subsystems are presented in detail below.

3.1 Increased aperture size

NPOI's current 12 cm individual feed apertures are being superseded with the installation of three 1.0 m telescopes. We have purchased three 'traditional' 1.0 m PlaneWave PW1000 telescopes (Figure 3), which are based upon lightweighted fused silica glass mirrors. These telescopes have all been delivered on-site, and currently two have been installed in their domes and are in operation.

3.2 Adaptive optics

Turnkey adaptive optics systems are now available commercially, and will be employed to fully utilize the light captured by the 1.0 m telescopes under a variety of seeing conditions. Both natural- and laser-guide-star systems are robust, operating reliably and rapidly [38]. We are currently developing two prototypes for first 'engineering' fringes, but will be pursuing commercial procurement of turnkey packages in the near future. Our first prototype is mounted on one of our PW1000's (Figure 4), with the second undergoing integration and test in the lab.

3.3 Beam feed

After wavefront correction, a collimated beam from our PW1000 telescopes will be routed along a PlaneWave-provided Coude train, and after relay mirror, into the existing NPOI beam train. At this point the interferometer is being a fed a collimated beam no different than its existing 12-cm beam feeds, and will combine 1-m telescope feeds without further modification.

3.4 Relocatable telescopes

The 1.0 m telescopes to be added to NPOI are housed in relocatable enclosure transporters ('ETs') (Figure 5), allowing for a variety of telescope separations. Each ET can be separated into 4 integral parts. First, a standard 16-foot AstroHaven dome encloses the telescope, protecting it against the elements. Second, a steel pedestal base has been built for mounting the telescope on; this base is roughly three feet in diameter and three feet high, weighing 1,500#.

Fig. 3: Lowell Observatory astronomers Drs. von Braun (left) and van Belle with one of the three PlaneWave PW1000 1-meter telescopes delivered to NPOI.

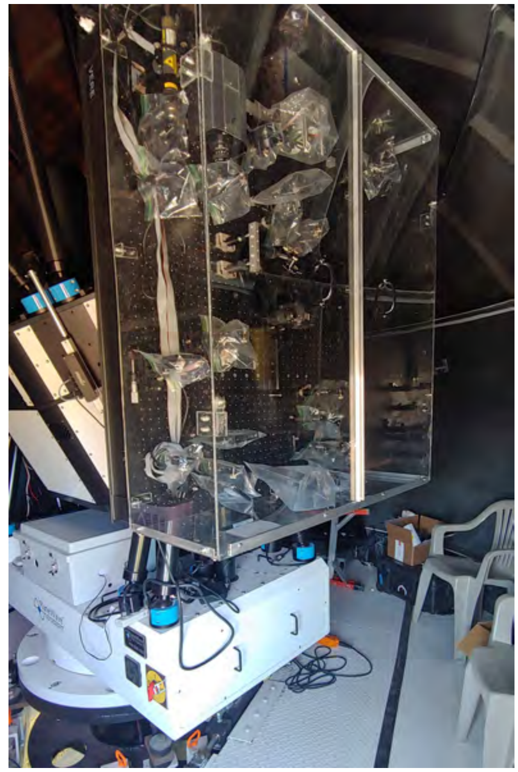

Fig. 4: Adaptive Optics breadboard # 1 (AO-1) mounted on a Nasmyth port for PW1000-1 at NPOI.

Fig. 5: Enclosure-Transporter (ET) units 2 (right) and 3 at NPOI.

Fig. 6: ET1 (left) after being moved to array center, with ET2 following, undergoing towing by our Bobcat.

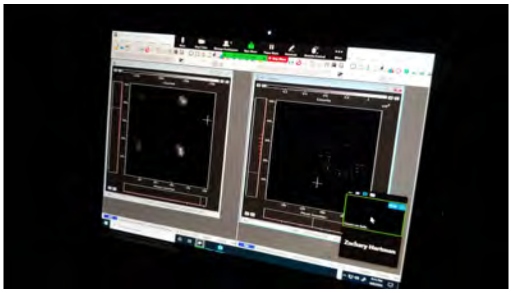

Fig. 7: First light for QWSSI; the four speckle imaging channels are seen on the left, with the wavefront sensor imager on the right.

Fig. 8: Dr. David Mozurkewich beginning the installation of the newNAT optical system.

Third, a hydraulic lift-lower mechanism allows the telescope and pedestal to be lifted for transport. Once lifted, the pedestal is mechanically locked into position for safety of the optical system during transport. Upon arrival at a new station, the locks are released, and the hydraulics bled to gently lower the pedestal and telescope; the bottom of the pedestal and top of the new station have a kinematic interface for positional repeatability. Finally, the trailer itself, with a pintle hitch, allows for the ET and its telescope to be moved around the NPOI site (Figure 6). Industry partner AstroHaven has provided Lowell with three ET units, which are assembled and on site. We have demonstrated moves of our PW1000-containing ET units around the site over distances of ∼one kilometer.

3.5 Short baseline stations

NPOI has stations with separations down to ∼8 m at the center of the array, and with the complementary use of speckle at the LDT, spacings below 4.3 m are obtained. Our currently operational 12-cm aperture stations allow for long baselines to be constructed out of short spacings; additional stations could be commissioned, optimized for the satellite observing case. At present we are developing two stations on a one ∼10 m baseline at array center for first fringes.

3.6 Baseline bootstrapping

A paradox of imaging with interferometry is that short baselines are needed to produce fringe visibilities significant enough to track, but long baselines, where fringes are too weak to track, are needed for high resolution imaging. The NPOI is designed to resolve this paradox by building medium to long baselines from a chain of shorter baselines, using the technique of baseline bootstrapping. Using the NPOI 12-cm apertures as operational pathfinder infrastructure, we have been pursuing on-sky demonstration of this technique [39] and in conjunction with coherent integration [35] to extend observation SNR.

3.7 Wavelength bootstrapping

Two essential benefits are gained from using near-IR light to fringe track. First, satellites are significantly brighter at near-infrared wavelengths; typical $V-J$ and $V-H$ colors are ∼3. [40]. A second benefit in the near-infrared is that, at longer wavelengths, fringe contrast increases. A useful technique is to cophase the array at a high SNR wavelength – in this case, the near-IR – but then take advantage of the cophased array and do imaging at a second, lower SNR wavelength – in this case, the visible. Additionally, the shorter wavelength for imaging provides greater spatial resolution.

Wavelength bootstrapping has already been demonstrated on-sky in a 'short-to-long' fashion at the VLTI, where 2.2 μm fringe tracking has increased the sensitivity of the 10 μm MIDI instrument by a factor of 20× [41]. However, it is important to note that converse 'long-to-short' technique of imaging from fringe tracking at K-band for V-band imaging has never been demonstrated on sky, and mature development of this technique represents a major technology deliverable of this work. Towards that end, we have been developing a near-infrared fringe tracker for NPOI [42] to provide IR cophasing for NPOI's visible-light VISION combiner [32].

3.8 Other subsystems

In addition to the above developments, existing infrastructure at NPOI continues to be updated with modern systems. This includes a new narrow-angle tracker for beam stabilization at the end of the interferometer beam train (newNAT, Figure 8), as well as completing the implementation of a modern fast delay line control system [4].

4. SUMMARY

Key high-altitude satellite imaging technologies is in the process of being demonstrated through the addition of large apertures and near-IR fringe-tracking hardware to the existing infrastructure of NPOI. NPOI is uniquely positioned for immediate demonstration of the necessary system engineering, integration & test, and on-sky demo of the baseline-wavelength bootstrapping technique with multiple apertures. Further significant retirement of system implementation risk could be achieved through demonstrating integration of a full compliment of six large apertures and an advanced near-IR fringe tracker at the NPOI facility. Direct demonstration of the accumulation of errors in the baseline-wavelength bootstrapping system for both wavelength-dependent phenomena (e.g. atmospheric DCR), independent phenomena (e.g. telescope motion), and other terms (e.g. influence of Strehl ratio) would guide design & implementation of a final operational system. Such a system scales naturally from the technology being developed at NPOI.

5. SAMPLE REFERENCES

[1] van Belle, G. et al. Developing Geostationary Satellite Imaging at the Navy Precision Optical Interferometer. In *Advanced Maui Optical and Space Surveillance Technologies Conference*, page 30, Jan. 2015.

[2] van Belle, G. Developing Geostationary Satellite Imaging at Lowell Observatory. In *Advanced Maui Optical and Space Surveillance Technologies Conference*, page 4, Sept. 2016.

[3] van Belle, G. Evolution in High Spatial Resolution Imaging of Faint, Complex Objects. In *Advanced Maui Optical and Space Surveillance (AMOS) Technologies Conference*, page 2, Jan. 2017.

[4] van Belle, G.T. et al. Many interesting things are afoot at the Navy Precision Optical Interferometer. In *Optical and Infrared Interferometry and Imaging VI*, volume 10701 of *Society of Photo-Optical Instrumentation Engineers (SPIE) Conference Series*, page 1070105, July 2018.

[5] Horch, E.P. et al. Observations of Binary Stars with the Differential Speckle Survey Instrument. I. Instrument Description and First Results. AJ, 137:5057–5067, June 2009.

[6] Horch, E.P. et al. Speckle Observations of Binary Stars with the WIYN Telescope. VII. Measures during 2008-2009. AJ, 143:10, Jan. 2012.

[7] Horch, E.P. et al. Observations of Binary Stars with the Differential Speckle Survey Instrument. IV. Observations of Kepler, CoRoT, and Hipparcos Stars from the Gemini North Telescope. AJ, 144:165, Dec. 2012.

[8] Horch, E.P. et al. Observations of Binary Stars with the Differential Speckle Survey Instrument. VI. Measures during 2014 at the Discovery Channel Telescope. AJ, 150(5):151, Nov. 2015.

[9] Furlan, E. et al. The Kepler Follow-up Observation Program. I. A Catalog of Companions to Kepler Stars from High-Resolution Imaging. AJ, 153(2):71, Feb. 2017.

[10] Kostov, V.B. et al. The L 98-59 System: Three Transiting, Terrestrial-size Planets Orbiting a Nearby M Dwarf. AJ, 158(1):32, July 2019.

[11] Horch, E.P. et al. Observations of Binary Stars with the Differential Speckle Survey Instrument. VIII. Measures of Metal-poor and Triple Stars from 2015 to 2018. AJ, 157(2):56, Feb. 2019.

[12] Horch, E.P. et al. Observations of Binary Stars with the Differential Speckle Survey Instrument. IX. Observations of Known and Suspected Binaries, and a Partial Survey of Be Stars. AJ, 159(5):233, May 2020.

[13] Calef, B., Therkildsen, E. and Roggemann, M.C. Wavefront-sensor-based frame selection. *Optical Engineering*, 44:116003, Nov. 2005.

[14] Calef, B. Speckle Imaging with a Partitioned Aperture: Laboratory Results. In *Advanced Maui Optical and Space Surveillance Technologies Conference*, page E12, Jan. 2009.

[15] Werth, M. et al. Multi-Frame Blind Deconvolution Accelerated with Graphical Processing Units (GPUs). In *Proceedings of the ¡A href="https://www.amostech.com"¿Advanced Maui Optical and Space Surveillance Technologies Conference¡/A*, page 5, Sept. 2019.

[16] Benson, J.A. et al. From fringes to the USNO Navy Prototype Optical Interferometer Astrometric Catalog. In *Society of Photo-Optical Instrumentation Engineers (SPIE) Conference Series*, volume 7734 of *Society of Photo-Optical Instrumentation Engineers (SPIE) Conference Series*, page 3, July 2010.

[17] Armstrong, J.T. et al. Detection of a geostationary satellite with the Navy Prototype Optical Interferometer. In *Society of Photo-Optical Instrumentation Engineers (SPIE) Conference Series*, volume 7734 of *Society of Photo-Optical Instrumentation Engineers (SPIE) Conference Series*, July 2010.

[18] Hindsley, R.B. et al. Navy Prototype Optical Interferometer observations of geosynchronous satellites. Appl. Opt., 50(17):2692, June 2011.

[19] Baines, E.K. et al. Navy Precision Optical Interferometer Measurements of 10 Stellar Oscillators. ApJ, 781:90, Feb. 2014.

[20] Kloppenborg, B.K. et al. Interferometry of $\in$ Aurigae: Characterization of the Asymmetric Eclipsing Disk. ApJS, 220(1):14, Sept. 2015.

[21] Cyr, R.P., Jones, C.E. and Tycner, C. Statistical Analysis of Interferometric Measurements of Axis Ratios for Classical Be Stars. ApJ, 799(1):33, Jan. 2015.

[22] Sigut, T.A.A. et al. The Circumstellar Disk of the Be Star o Aquarii as Constrained by Simultaneous Spectroscopy and Optical Interferometry. ApJ, 814(2):159, Dec. 2015.

[23] Hutter, D.J. et al. Surveying the Bright Stars by Optical Interferometry. I. A Search for Multiplicity among Stars of Spectral Types F-K. ApJS, 227(1):4, Nov. 2016.

[24] Jones, C.E. et al. The Disk Physical Conditions of 48 Persei Constrained by Contemporaneous Hα Spectroscopy and Interferometry. ApJ, 843(1):24, July 2017.

[25] Baines, E.K. et al. Fundamental Parameters of 87 Stars from the Navy Precision Optical Interferometer. AJ, 155(1):30, Jan. 2018.

[26] Mourard, D. et al. Physical properties of β Lyrae A and its opaque accretion disk. A&A, 618:A112, Oct. 2018.

[27] Armstrong, J.T. et al. Interferometric Fringe Visibility Null as a Function of Spatial Frequency: A Probe of Stellar Atmospheres. *Journal of Astronomical Instrumentation*, 8(4):1950012–246, Jan. 2019.

[28] Hutter, D.J. et al. Surveying the Bright Stars by Optical Interferometry. II. A Volume-limited Multiplicity Survey of Main-sequence F Stars. ApJS, 243(2):32, Aug. 2019.

[29] Suffak, M.W. et al. The Large-scale Behavior in the Disk of δ Scorpii from 2000 to 2018. ApJ, 890(1):86, Feb. 2020.

[30] Sigut, T.A.A., Mahjour, A.K. and Tycner, C. Stellar Inclination Angles from Be-star Hα Emission Line Profiles. ApJ, 894(1):18, May 2020.

[31] Ghasempour, A. et al. Building the next-generation science camera for the Navy Optical Interferometer. In *Society of Photo-Optical Instrumentation Engineers (SPIE) Conference Series*, volume 8445 of *Society of Photo-Optical Instrumentation Engineers (SPIE) Conference Series*, page 0, July 2012.

[32] Garcia, E.V. et al. Vision: A Six-telescope Fiber-fed Visible Light Beam Combiner for the Navy Precision Optical Interferometer. PASP, 128(963):055004, May 2016.

[33] Armstrong, J.T. et al. Precise stellar diameters from coherently averaged visibilities. In *Society of Photo-Optical Instrumentation Engineers (SPIE) Conference Series*, volume 8445 of *Society of Photo-Optical Instrumentation Engineers (SPIE) Conference Series*, page 3, July 2012.

[34] Jorgensen, A.M. et al. Progress toward unprecedented imaging of stellar surfaces with the Navy precision optical interferometer. In *Society of Photo-Optical Instrumentation Engineers (SPIE) Conference Series*, volume 9146 of *Society of Photo-Optical Instrumentation Engineers (SPIE) Conference Series*, page 0, July 2014.

[35] Mozurkewich, D., Jorgensen, A. and van Belle, G.T. Coherent Integration in Astronomical Interferometry: Theory and Practice. *Journal of Astronomical Instrumentation*, 8(2):1950005, Jan. 2019.

[36] Armstrong, J.T. et al. The Navy Prototype Optical Interferometer. ApJ, 496:550, Mar. 1998.

[37] Armstrong, J.T. et al. The Navy Precision Optical Interferometer (npoi): AN Update. *Journal of Astronomical Instrumentation*, 2:40002, Dec. 2013.

[38] Baranec, C. et al. High-efficiency Autonomous Laser Adaptive Optics. ApJ, 790:L8, July 2014.

[39] Jorgensen, A.M. et al. Multi-baseline chain bootstrapping with new classic at the NPOI. In *Optical and Infrared Interferometry and Imaging V*, volume 9907 of *Society of Photo-Optical Instrumentation Engineers (SPIE) Conference Series*, page 99072C, Aug. 2016.

[40] Sanchez, D.J. et al. Photometric measurements of deep space satellites. In Bilbro, J.W. et al, editors, *Imaging Technology and Telescopes*, volume 4091 of *Society of Photo-Optical Instrumentation Engineers (SPIE) Conference Series*, pages 164–182, Oct. 2000.

[41] Müller, A. et al. First results using PRIMA FSU as a fringe tracker for MIDI. In *Society of Photo-Optical Instrumentation Engineers (SPIE) Conference Series*, volume 7734 of *Society of Photo-Optical Instrumentation Engineers (SPIE) Conference Series*, July 2010.

[42] Armstrong, J.T. et al. An infrared beam combiner for wavelength bootstrapping at the NPOI. In *Optical and Infrared Interferometry and Imaging VI*, volume 10701 of *Society of Photo-Optical Instrumentation Engineers (SPIE) Conference Series*, page 107010B, July 2018.